



# Cryptic hybridization between the ancient lineages of Natterer's bat (*Myotis nattereri*)

Darija Josić<sup>1</sup>  | Emrah Çoraman<sup>2</sup> | Isabelle Waurick<sup>1</sup> | Sören Franzenburg<sup>3</sup> | Leonardo Ancillotto<sup>4</sup> | Branka Bajić<sup>5</sup> | Ivana Budinski<sup>5</sup> | Christian Dietz<sup>6</sup> | Tamás Görföl<sup>7,8</sup> | Sofia I. Hayden Bofill<sup>1</sup> | Primož Presetnik<sup>9</sup> | Danilo Russo<sup>4</sup> | Martina Spada<sup>10</sup> | Vida Zrnčić<sup>11</sup> | Mozes P. K. Blom<sup>1</sup> | Frieder Mayer<sup>1,12</sup> 

<sup>1</sup>Museum für Naturkunde, Leibniz Institute for Evolution and Biodiversity Science, Berlin, Germany

<sup>2</sup>Department of Ecology and Evolution, Eurasia Institute of Earth Sciences, Istanbul Technical University, İstanbul, Türkiye

<sup>3</sup>IKMB, Institute of Clinical Molecular Biology, University of Kiel, Kiel, Germany

<sup>4</sup>Laboratory of Animal Ecology and Evolution (AnEcoEvo), Dipartimento di Agraria, Università degli Studi di Napoli Federico II, Portici, Italy

<sup>5</sup>Department of Genetic Research, Institute for Biological Research 'Siniša Stanković' – National Institute of Republic of Serbia, University of Belgrade, Belgrade, Serbia

<sup>6</sup>Biologische Gutachten Dietz, Haigerloch, Germany

<sup>7</sup>Department of Zoology, Hungarian Natural History Museum, Budapest, Hungary

<sup>8</sup>National Laboratory of Virology, University of Pécs, Pécs, Hungary

<sup>9</sup>Centre for Cartography of Fauna and Flora, Miklavž na Dravskem Polju, Slovenia

<sup>10</sup>Dipartimento Ambiente-Salute-Sicurezza, Università degli Studi dell'Insubria, Varese, Italy

<sup>11</sup>Croatian Biospeleological Society Zagreb, Zagreb, Croatia

<sup>12</sup>Berlin-Brandenburg Institute of Advanced Biodiversity Research (BBIB), Berlin, Germany

## Correspondence

Darija Josić and Frieder Mayer, Museum für Naturkunde, Leibniz Institute for Evolution and Biodiversity Science, Berlin, Germany.

Email: [josic.darija@gmail.com](mailto:josic.darija@gmail.com) and [frieder.mayer@mfn.berlin](mailto:frieder.mayer@mfn.berlin)

## Funding information

National Research, Development, and Innovation Fund of Hungary, Grant/Award Number: NKFIH FK137778 and RRF-2.3.1-21-2022-00010; Deutsche Forschungsgemeinschaft, Grant/Award Number: 407495230 and 423957469; János Bolyai Research Scholarship of the Hungarian Academy of Sciences, Grant/Award Number: BO/00825/21; Elsa-Neumann-Scholarship; Leibniz Association, Grant/Award Number: K309/2020

Handling Editor: Alana Alexander

## Abstract

Studying hybrid zones that form between morphologically cryptic taxa offers valuable insights into the mechanisms of cryptic speciation and the evolution of reproductive barriers. Although hybrid zones have long been the focus of evolutionary studies, the awareness of cryptic hybrid zones increased recently due to rapidly growing evidence of biological diversity lacking obvious phenotypic differentiation. The characterization of cryptic hybrid zones with genome-wide analysis is in its early stages and offers new perspectives for studying population admixture and thus the impact of gene flow. In this study, we investigate the population genomics of the *Myotis nattereri* complex in one of its secondary contact zones, where a putative hybrid zone is formed between two of its cryptic lineages. By utilizing a whole-genome shotgun sequencing approach, we aim to characterize this cryptic hybrid zone in detail. Demographic analysis suggests that the cryptic lineages diverged during the Pliocene, c. 3.6 million years ago. Despite this ancient separation, the populations in the contact zone exhibit mitochondrial introgression and a considerable amount of mixing in nuclear genomes. The genomic structure of the populations corresponds to geographic locations and

This is an open access article under the terms of the [Creative Commons Attribution-NonCommercial-NoDerivs](https://creativecommons.org/licenses/by-nc-nd/4.0/) License, which permits use and distribution in any medium, provided the original work is properly cited, the use is non-commercial and no modifications or adaptations are made.

© 2024 The Author(s). *Molecular Ecology* published by John Wiley & Sons Ltd.

the genomic admixture changes along a geographic gradient. These findings suggest that there is no effective hybridization barrier between both lineages, nevertheless, their population structure is shaped by dispersal barriers. Our findings highlight how such deeply diverged cryptic lineages can still readily hybridize in secondary contact.

#### KEYWORDS

bats, introgression, secondary contact, speciation

## 1 | INTRODUCTION

The isolation of nuclear genomes is rather frequently incomplete across eukaryote species, allowing hybridization among populations with wide-ranging effects on adaptation and speciation (Barth et al., 2020). Hybridization after secondary contact can produce contrasting outcomes depending on the extent and the level of genetic differentiation and/or the accumulation of reproductive barriers during isolation. On the one hand, secondary contact can decrease the level of genetic differentiation or even lead to the fusion of gene pools by rapidly eroding the barriers to gene exchange; on the other, reinforcement may strengthen premating reproductive barriers in the case of selection against hybrids (Baiz et al., 2019; Barton & Hewitt, 1985; Seehausen, 2006; Wu, 2001). Empirical studies of secondary contact zones have shown that the nature and extent of reproductive isolation vary across sister species pairs, ranging from substantial pre- and post-zygotic isolation (Alexandrino et al., 2005; Kindler et al., 2017; Leaché & Cole, 2007; Phillips et al., 2004) to genetic fusion with few barriers to the neutral dispersal of alleles (Sequeira et al., 2005; Singhal & Moritz, 2013; Wake & Schneider, 1998). An increasing number of studies have identified stable, long-lasting natural hybrid zones, suggesting that varying degrees of reproductive isolation can be maintained despite the potential homogenizing effects of gene flow across larger geographic distances (Abbott et al., 2013; Barton & Hewitt, 1985; Hewitt, 1988; Moore, 1977).

Until recently, secondary contact zone studies mostly focused on morphologically distinct taxa while much less is known about the contact zones of cryptic lineages (Slager et al., 2020). The accumulation of genetic data, on the other hand, suggests that there is substantial cryptic diversity in various taxonomic groups (Struck et al., 2018). Bats, for instance, have become a prominent example because of their extraordinary cryptic diversity, initiated by the discovery of highly differentiated mitochondrial lineages (e.g. Clare et al., 2011; Çoraman et al., 2013; Mayer et al., 2007). This is not surprising since the traits important for species recognition and mate choice in bats, such as ultrasound communication calls and olfactory cues, are challenging to study and hence identifying potential differences is considerably difficult. Furthermore, bats are rather inconspicuous in their colouration and closely related species usually have relatively similar appearances. In the last couple of decades, several bat populations represented by divergent mitochondrial lineages were described as new taxa, including new

species. However, several cases of cyto-nuclear conflicts were reported indicating at least occasional introgression of mitochondrial genomes (e.g. Artyushin et al., 2009; Berthier et al., 2006; Çoraman et al., 2019, 2020; Furman et al., 2014; Mao & Rossiter, 2020). These studies were mostly based on mitochondrial DNA and sometimes included very few nuclear markers with limited phylogenetic resolution. More importantly, individuals from contact zones were rarely studied and thus little is known about the ongoing patterns of gene flow between lineages.

In this study, we investigate the population genomic structure in one of the secondary contact zones of a cryptic bat complex: *Myotis nattereri* sensu lato. The *M. nattereri* complex is one of the most genetically diverse groups of bats and has received much attention because of its deeply diverged cryptic lineages. In the last 15 years, the widely distributed *M. nattereri* sensu lato was successively split into several taxa, largely based on the genetically divergent lineages; *M. nattereri* sensu stricto, *M. escalerae* in the Iberian Peninsula (Ibáñez et al., 2006), *M. crypticus* in the Apennine Peninsula (Juste et al., 2018; Ruedi et al., 2019: but see Çoraman et al., 2019), *M. zenatius* in Morocco and Algeria (Juste et al., 2018; Ruedi et al., 2019: but see Çoraman et al., 2019), *M. tschuliensis* in the Caucasus, the northwestern coast of Black Sea and the Kopet Dag Mountains in Turkmenistan (Çoraman et al., 2019; Kruskop & Solovyeva, 2020), *Myotis nustrale* in Corsica (Puechmaillie et al., 2023) and finally, *M. hoveii* in the Levant region (Çoraman et al., 2019; Smirnov et al., 2020; Uvizl & Benda, 2021). Although these taxa are highly differentiated at the mitochondrial genome, they closely resemble each other in morphology and are mostly indistinguishable in external characters. Based on the dense genetic sampling, the distribution ranges of these taxa are now well understood and several cryptic contact zones have been identified. However, nothing is known about reproductive isolation between cryptic lineages and thus the extent of gene flow and hybridization upon secondary contact. Recently, based on the analysis of one mitochondrial gene and four nuclear intron markers, Çoraman et al. (2019) found several cytonuclear conflicts indicating multiple hybridization events between some of these cryptic lineages. However, the timing and the extent of these hybridization events remained unknown.

The focus of this study is the secondary contact zone of two cryptic lineages in an area encompassing the eastern Alps and the northwest of the Balkan Peninsula (Figure 1a), a well-known area of post-glacial secondary contact zones of animals and plants

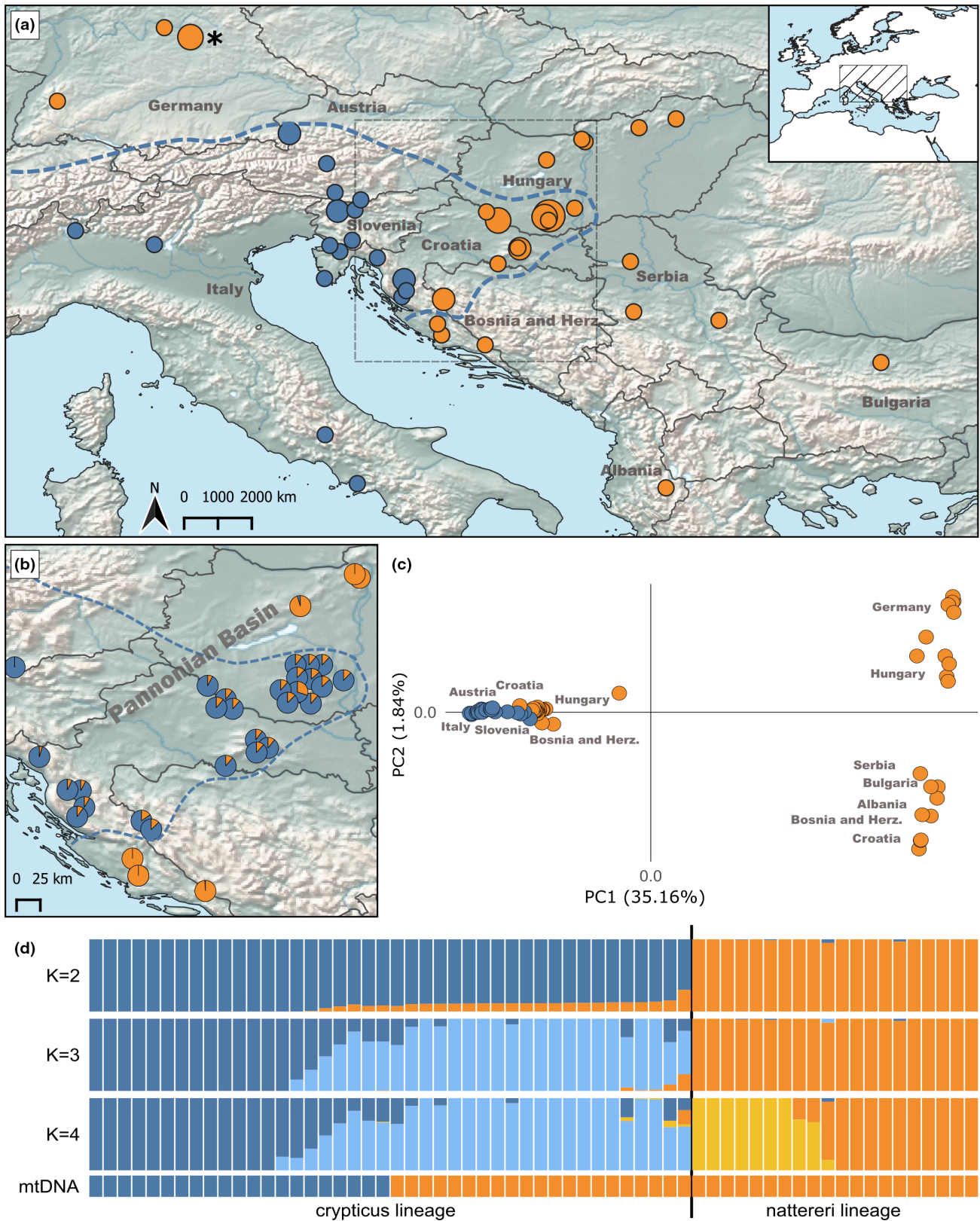


**FIGURE 1** (a) Sampling locations. Individuals were coloured by their mitochondrial DNA: Blue for crypticus and orange for nattereri. The size of a point indicates the number of samples at a location. The dashed line approximates the border between individuals with a predominantly crypticus or nattereri nuclear genome. The individual from southern Bavaria marked with an asterisk exhibited an admixed genome. (b) Focus on the hybridization zone. Pie charts indicate the admixture proportions for each individual. (c) PC plot obtained using genotype likelihoods. (d) Admixture panels showing clusters for  $K$  between 2 and 4. Individuals were sorted according to admixture proportion for  $K=2$ . The lower panel shows the assignment of individuals to mitochondrial lineages.

(Hewitt, 2000; Taberlet et al., 1998). Çoraman et al. (2019) found that some of the individuals from this area had cytonuclear discordance and they interpreted this as caused by the mitochondrial introgression from the local nattereri populations (hereafter referred to as the nattereri lineage) to the expanding populations of crypticus (hereafter referred to as the crypticus lineage) from the Apennine Peninsula. Based on the timing of this expansion, they suggested that these lineages recently came into secondary contact after the Last Glacial Maximum. These interpretations were based on relatively few nuclear and mitochondrial markers, and the level and the timing of gene flow between these lineages remained unexplored. Here, we utilized a whole-genome shotgun sequencing approach, and we explored the whole-genome differentiation of these lineages. Our main aims are (i) to investigate whether and to which degree the two lineages hybridized or still hybridize, (ii) to localize and characterize the hybrid zone and (iii) to estimate the divergence time of the two lineages using demographic approaches. Being one of the first studies to apply a whole-genome approach in a bat secondary contact zone, this study will contribute to the understanding of the evolutionary consequences of hybridization such as range expansion, genomic introgression and adaptation.

## 2 | MATERIALS AND METHODS

### 2.1 | Sampling

Samples were obtained from the collection at the Museum für Naturkunde Berlin or recent fieldwork (Table S1). Wild bats were caught using mist nets. After species identification, age and sex were determined and external morphological traits were measured. In addition, a small wing sample of 3–5 mm in diameter was taken by a sterile biopsy punch and stored in 80% ethanol. After processing, each bat was immediately released at the capture site. In total, the genomes of 62 bats were sequenced originating from 46 locations in 10 countries comprising Italy, Slovenia, Austria, Croatia, Hungary, Bosnia and Herzegovina, Serbia, Albania, Bulgaria and Germany (Figure 1a).

### 2.2 | DNA extraction

DNA was extracted either by using QIAGEN DNeasy Blood and Tissue kit following the manufacturer's recommendation or with a salt–chloroform extraction method (Dietz et al., 2016; Müllenbach et al., 1989). Tissue samples were digested in a lysis buffer for 1 h at 56°C, followed by 37°C overnight. In the end, DNA was eluted in 90 µL of AE buffer (Qiagen). We checked the DNA concentration and purity by using a NanoDrop spectrophotometer (Thermo Fisher Scientific Inc). The degree of DNA degradation was visualized by agarose gel (1%) electrophoresis.

For genomic library preparation, 500 ng of DNA was mechanically sheared by an S220 Focused Ultrasonicator (Covaris

Inc) to achieve a fragment length below 800 bp. The fragment size distribution of sheared DNA was checked with Bioanalyzer (High Sensitivity DNA Chip, Agilent Inc) and concentration was determined using Qubit 2.0 Fluorometer and dsDNA HS Assay Kit (Thermo Fisher Scientific Inc). Eighty nanogram of fragmented DNA was used to prepare libraries for paired-end Illumina sequencing with NEXTflex Rapid DNA Seq Kit 2.0 (PerkinElmer Inc) (Table S2).

During the study, a switch was made to the NEXTflex Rapid XP Library Preparation Kit (PerkinElmer Inc) employing an enzymatic fragmentation. One-hundred nanogram of unshredded DNA was used for preparing Illumina libraries (Table S2).

### 2.3 | Genome shotgun sequencing

In total, three different NEXTFLEX library preparation kits (PerkinElmer Inc) were used following the manufacturer's instructions: NEXTflex Rapid XP DNaseq Kit for 45 enzymatically sheared samples, NEXTflex Rapid DNaseq Kit for 6 mechanically sheared samples and NEXTflex Rapid DNaseq Kit 2.0 for 11 mechanically sheared samples. All libraries were made according to the manufacturer's 'bead size selection' protocol aiming for a library size of ~500 bp and libraries were barcoded for multiplexing with NEXTflex HT Barcodes (PerkinElmer Inc).

Library size and quantity were determined with a Bioanalyzer or a TapeStation (High Sensitivity DNA Chip or D1000 Kit, Agilent Technologies Inc) and a Qubit 2.0 Fluorometer (dsDNA HS Assay Kit, Thermo Fisher Scientific Inc) following the manufacturer's recommendations.

Genomic libraries were all sequenced at 150 bp paired end on three different Illumina sequencing instruments NextSeq500, HiSeq2500 and NovaSeq6000. Five samples were additionally sequenced as 150 bp single end on a NextSeq500 instrument (Table S2).

### 2.4 | Merging and cleaning reads

Following sequencing, the quality of raw reads was inspected with FastQC v0.11.8 (Andrews, 2010) after which the adapters were removed using Trimmomatic v0.36 (Bolger et al., 2014). Overlapping reads were then merged using PEAR v0.9.11 (Zhang et al., 2014). The p-value for the assembly using PEAR had to exceed the lowest possible value of 0.0001, the minimum overlap size had to be at least 20 bp and a minimum possible read length of 30 bp was required. Next, quality trimming was done by Trimmomatic v0.36 (Bolger et al., 2014) to trim read ends with phred base quality below 15 and to discard reads shorter than 30 bp. Following cleaning, the polished reads data were then re-checked with FastQC v0.11.8 to ensure that all possible adapters and low-quality sequences were removed. Parameters not mentioned in this section were left at their default or as recommended in the programs' manuals.



## 2.5 | Mapping to the *Myotis myotis* reference genome

We mapped the cleaned reads to the *M. myotis* reference genome (GenBank assembly accession: GCA\_014108235.1) that was provided by the Bat1K genome project allowing us early access to the non-annotated 92 scaffold assembly (Jebb et al., 2020). We used Burrows-Wheeler Aligner (Li & Durbin, 2009) BWA v0.7.17 mem algorithm, using the -M parameter to ensure compatibility with Picard Tools ([broadinstitute.github.io/picard/](https://broadinstitute.github.io/picard/)). Both paired and unpaired reads were mapped separately to produce a bam (binary alignment) file for each individual. We used Picard Tools MarkDuplicates v2.18.25 to remove duplicates. We then used samtools-1.9 (Li et al., 2009) to sort and merge the bam files with paired and unpaired reads. After merging, we used Qualimap v2.2.1 (Okonechnikov et al., 2016) to evaluate the mapping results for each individual.

## 2.6 | Variant calling

We used two parallel workflows for variant calling, using hard-called genotypes and genotype likelihoods to assess whether the heterogeneity in coverage between samples (Table S1) influenced the inference of population structure.

For the pipeline based on genotypes, we used Freebayes v1.3.1 (Garrison & Marth, 2012). Only reads with a mapping quality score above 10 were used to generate a multi-sample VCF file. Subsequently, we filtered with VCFtools v0.1.17 (Danecek et al., 2011) using the following parameters: only biallelic sites, coverage per site between 2 and 40 for each individual and mean coverage between 5 and 60 over all included individuals. Minimal mapping quality was set to 20, and we allowed for 10% missing data per site. Finally, indels were removed and the minor allele frequency threshold was set to 0.03.

Genotype likelihoods (GLs) were estimated using the GATK model in ANGSD v0.928 (Korneliusson et al., 2014; McKenna et al., 2010), which only uses the observed bases that overlap at a specific position together with their associated sequencing quality scores. Only sites with a minimum mapping quality of 20 and minimum coverage of 2 were considered. The SNP  $p$ -value threshold for the likelihood ratio test was set to  $1e-6$ . We excluded sites that showed a significant  $p$ -value for being triallelic, and those that had a minor allele frequency below 0.05.

## 2.7 | Relatedness

We applied NgsRelate v.2 (Hanghøj et al., 2019) to infer relatedness using genotype likelihoods within our nattereri and crypticus individuals. As input for this, we calculated genotype likelihoods of our dataset using ANGSD as described previously with the addition of -doGlf 3 which prints the output as a binary likelihood file as opposed to a beagle file. The number of sites used between pairwise comparisons was 48,859,081 for nattereri individuals and 53,864,885 for crypticus individuals.

## 2.8 | Population structure analysis

To assess population genetic structure, we performed a principal component analysis (PCA) first on hard-called autosomal genotypes and second on genotype likelihoods. The PCA on genotypes was performed using Plink-1.9 (Chang et al., 2015). To account for non-independence between sites (linkage disequilibrium; LD), we pruned all sites with an  $r^2$  exceeding 0.1 across a 50 kb window. The PCA using genotype likelihoods for the whole genome was performed by PCAngsd v0.98 (Meisner & Albrechtsen, 2018).

## 2.9 | Admixture analysis

To further analyse the population structure and to identify admixed individuals, we performed admixture analyses on both the genotype and the genotype likelihood data set comprising all 62 individuals.

The genotype data set was analysed using the Admixture v1.3.0 software (Alexander et al., 2009). We varied the number of possible populations (K) between 1 and 10. The best-supported value of K was determined using the lowest value of the cross-validation error in Admixture.

The admixture analysis based on genotype likelihoods was performed with NGSAdmix v32 (Skotte et al., 2013). We ran NGSAdmix five times with K ranging between 1 and 10, and the rest of the settings were left as default. The optimal value for K was determined by the delta K statistic (Evanno et al., 2005), which was calculated from the obtained log-likelihood scores with CLUMPAK (Kopelman et al., 2015).

Individuals were assigned to three different categories according to the results of the Admixture and the NGSAdmix analyses for  $K=2$ . Individuals being assigned by both analyses as 100% to only one group were classified as 'pure nattereri' or 'pure crypticus'. Individuals with admixture proportions to both groups were classified as 'admixed'.

## 2.10 | Population differentiation and ancestry informative markers (AIMs)

The pairwise per site fixation index ( $F_{ST}$ ) was calculated between nattereri and crypticus individuals based on genotypes from the Freebayes pipeline using the software VCFtools (-weir-fst-pop option).

To further evaluate the degree of admixture of candidate hybrids, we first identified loci with fixed differences between 'pure nattereri' and 'pure crypticus'. We identified sites with an  $F_{ST}$  value of 1, that is, fixed differences, by comparing non-admixed (pure) individuals of the two parental populations. Subsequently, we asked for each of these ancestry informative markers (sites) whether an admixed individual was homozygous for the nattereri allele, heterozygous or homozygous for the crypticus allele. Based on these genotypes, we calculated for each admixed individual its hybrid index and

heterozygosity (Figure 2). For evaluating the hybridization ancestry of admixed individuals, we calculated the expected hybrid index and heterozygosity for an  $F_1$ ,  $F_2$  and a first-generation backcross hybrid for two scenarios. First, hybrids originating from mating between a pure nattereri and pure crypticus. Second, for the hybridization scenario between a pure nattereri and an individual from the admixed Hungarian population in the Pannonian basin with 15% nattereri and 85% crypticus ancestry. Finally, the hybrid index and heterozygosity were calculated for an individual from a panmictic hybrid population with 15% nattereri and 85% crypticus ancestry (Figure 2).

We used the GenoPop R package (<https://github.com/MiGurke/GenoPop>) to calculate nucleotide diversity ( $\pi$ ) within each pure population and nucleotide divergence between the two pure populations ( $D_{xy}$ ). We used the same R package to calculate the  $F_{ST}$ ,  $\pi$  and  $D_{xy}$  across the whole genome in 50kb and 100kb windows with a 1000kb step.

## 2.11 | Demographic analyses

The demographic history of both pure populations was inferred using the pairwise sequentially Markovian coalescent (PSMC) model (Li & Durbin, 2011) and coalescent-based simulations implemented

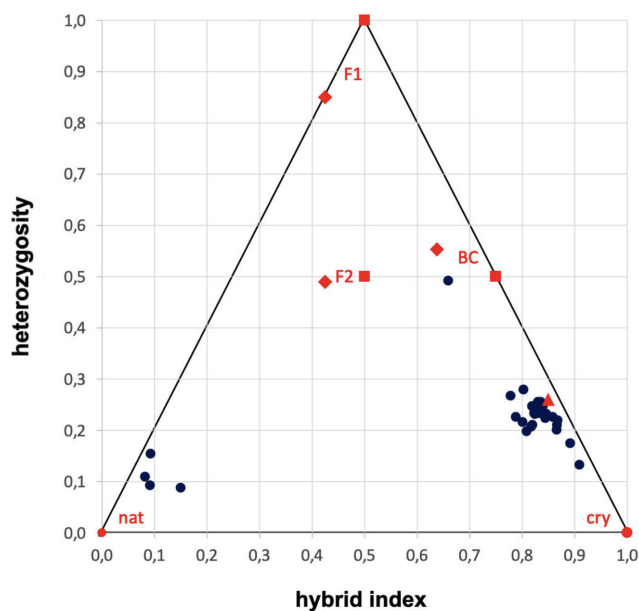


**FIGURE 2** Triangle plot of admixed individuals based on hybrid index and heterozygosity both calculated by fixed sites from the AIM analysis (blue circles). Red circles refer to expected values of pure nattereri and crypticus individuals. Red squares represent expected values of an  $F_1$  hybrid or an  $F_2$  hybrid or a first-generation backcross to a pure crypticus individual. Red rhombs represent expected values of an  $F_1$  hybrid between a pure nattereri and an admixed individual with 15% nattereri and 85% crypticus ancestry or an  $F_2$  hybrid or a first-generation backcross to an admixed individual with 15% nattereri and 85% crypticus ancestry. Red triangle represents the expected value of an individual of a panmictic population of 15% nattereri and 85% crypticus ancestry.

in Fastsimcoal2 (Excoffier et al., 2021). For PSMC analysis, we used three high-coverage genomes: two samples of crypticus (representing two lineages according to Çoraman et al., 2019) and one sample of nattereri from southern Germany. We applied the PSMC model to the autosomal sequences. A consensus diploid sequence for each individual was generated by using the mpileup command in BCFtools v1.9 (Li, 2011), with the BAM file as an input and *M. myotis* as a reference, while adjusting for mapping quality ( $-C$  50). The X chromosome was excluded by using a BED file without scaffold 4 when running a mpileup. The output was then passed to BCFtools to construct the actual consensus sequence using the  $-c$  flag. This consensus VCF file was then converted to fastq format using the vcf2fq command of the vcfutils script and setting the minimum read depth ( $-d$ ) to 12 and maximum read depth ( $-D$ ) to 100. Finally, the consensus sequence in fastq format was converted to the input format required by PSMC using the fq2psmcfa script provided by PSMC, while filtering out bases with a quality score lower than 20. PSMC analysis was run using the parameter settings  $-t$  15  $-r$  5  $-p$  4+25  $\times$  2+4+6, as previously reported by Chattopadhyay et al. (2019). One hundred bootstrap replicates were performed for each of the three samples.

In addition, we used the composite-likelihood method implemented in Fastsimcoal2 v2.7 (Excoffier et al., 2021) to evaluate five alternative demographic models (no, early, different, constant and recent gene flow, Figure 4, Table S3) by including all individuals. To prepare the input site frequency spectrum (SFS) for Fastsimcoal2, we used a VCF file that had no MAF filter applied. All other filters were the same as for the VCF file that was used for hard calling and PCA. We used EasySFS (<https://github.com/isaacovercast/easySFS#easysfs>) to convert variant call format (VCF) to the Fastsimcoal2 style site frequency spectrum. In the preparation of the SFS, we adjusted the genome sequence length in the following way. Given that filtering was applied only to the raw VCF file (variant sites only), we assumed the same sequence quality for variant and monomorphic sites. Accordingly, the genome size was reduced by the proportion of SNPs that were filtered out from the raw VCF file.

We ran each model 100 times with 80 iterations per run for likelihood maximization. The expected site frequency spectrum (SFS) was approximated through 250,000 coalescent simulations per iteration. We assumed a mutation rate of  $2.5 \times 10^{-8}$  per bp per haploid genome per generation. No population growth was allowed, but population size could change when migration rates changed. The best model was selected according to the Akaike information criterion (AIC, Akaike, 1974). To obtain 95% confidence intervals (CI) for best model parameters, we used a non-parametric block-bootstrap approach. We split our VCF file into 100 parts that we then randomly put back together. We created 50 new VCF files and we then reran Fastsimcoal2 as described above for each of these VCFs. We followed the steps described here: <https://speciationgenomics.github.io/fastsimcoal2/>. We used the parameter estimates from the best run of each VCF to calculate our 95% CI.

For both demographic analyses, we used a mutation rate of the human genome of  $2.5 \times 10^{-8}$  mutations per nucleotide site per

generation (Sovic et al., 2016) and a generation time of 7.3 years, which was estimated for the closely related species *Myotis bechsteinii* (Fleischer et al., 2017).

## 2.12 | Nuclear phylogenetics

To infer a nuclear phylogeny, we first called variants with FreeBayes v1.3.1 (Garrison & Marth, 2012) for each individual and scaffold. Only variants with a quality score above 20 were retained and indel variation was removed. We then used SAMtools v1.12 (Li et al., 2009) to calculate coverage depth at each position and generated a mask file for consensus calling with BCFtools (Li, 2011). The resulting consensus sequences for each scaffold and individual included N's at sites that were either heterozygous, or had a coverage below 3 or higher than 150x. The consensus sequences were combined into alignments for each scaffold and filtered using a custom Python script. We used a jumping window approach where we sampled a window of 10kb long and every 300kb, and assessed the extent of missing data for that specific window. Alignment columns with more than 50% missing data were removed and windows were discarded if less than 50% of the alignment columns remained. Moreover, each alignment row (individual) needed to have less than 40% missing data and windows were only retained when more than 80% of our target individuals fulfilled those criteria. If a window did not pass these filtering criteria, a window alignment directly adjacent to that window was sampled and again filtered for the same criteria. We used the window alignments for two distinct phylogenetic approaches. First, we concatenated all window alignments into one large genome alignment (sex-linked scaffold 4 was excluded) and inferred a maximum-likelihood phylogeny using IQtree2 v2.0.3 (Minh et al., 2020) and a GTR+I+G substitution model. To assess bipartition support, we used ultra-fast bootstrapping as implemented in IQtree2 with 1000 replicates. Second, to account for incomplete lineage sorting, we inferred a maximum-likelihood 'gene'-tree (IQtree2) for each of the window alignments and then used a summary coalescent approach to infer a species tree using ASTRALIII (Zhang et al., 2018). We used IQtree2 to evaluate bipartition support by calculating site and window concordance factors using all window alignments and trees.

## 2.13 | Mitochondrial phylogenetics

Mitochondrial genomes were assembled by mapping the cleaned reads to the *M. myotis* (RefSeq: NC\_029346) mitochondrial genome (Jebb, Foley, Puechmaille, & Teeling, 2017). We used the BWA-mem algorithm for mapping all acquired reads to the mitochondrial genome requiring a mapping quality above 20. We used FreeBayes to call variants and GATK v4.1.3.0 FastaAlternateReference maker (Van der Auwera et al., 2013) was used to generate consensus sequences for each individual. Sites were masked if coverage was below 10 or above 5 times the mean coverage. A multiple-sequence alignment was generated by using the G-insi algorithm in MAFFT (Kato &

Standley, 2013), and no evidence for nuclear mitochondrial DNA (numts), premature stop codons and frameshifts was found by visual inspection of the alignment in Geneious 2019.2.3 (Biomatters Ltd). The mitochondrial genome of *M. bechsteinii* (RefSeq: NC\_034227.1; Jebb, Foley, Kerth, & Teeling, 2017) was included in the alignment as an outgroup. A maximum-likelihood phylogeny was inferred using RAxML v8.2.10 (Stamatakis, 2014) by identifying the tree with the highest likelihood score out of 10 independent tree searches and 100 bootstrap replicates were conducted to estimate support.

## 3 | RESULTS

### 3.1 | Genome sequencing and variant calling

Sequencing of 62 individuals was done in two batches and differed in sequencing yield (Table S1). Among the 59 individuals sequenced at a lower depth, we retained 44,363,594 to 255,125,812 (mean 117,499,668) reads per individual; between 57% and 98% (mean 78%) of all reads were kept after filtering. All retained reads were mapped to the reference nuclear genome and the reference mitochondrial genome of *Myotis myotis*. Between 97% and 99% (mean 98%) of these reads mapped successfully to the nuclear genome and mapping quality varied between 48 and 53 (mean 52). Sequencing coverage of the nuclear genome ranged from 2.5x to 12.8x with a mean of 6.7x. In addition, three individuals were sequenced at a higher depth to perform a PSMC analysis (Table S1). Sequencing coverage of the nuclear genome of these three individuals was 27.4x, 34.5x and 36.0x. After calling and filtering variants, we obtained 25,788,685 SNPs with FreeBayes and VCFtools, while using ANGSD and genotype likelihoods, we obtained 33,640,565 SNPs.

### 3.2 | Population structure

Our results using NgsRelate show that individuals were not related. Population structure analysis using principal component analyses (PCAs) revealed two clearly separated groups, that is, the nattereri and crypticus lineages, irrespective of the approach used. Principal component 1 (PC1) separates the two lineages while using both methodological approaches (i.e. genotype likelihoods (Figure 1c) and hard calling of genotypes (Figure S1a)), explaining 35.2% and 33.8%, respectively, of the total variance. The two groups split according to the taxonomy of individuals from outside a putative contact zone. One group comprises all the nattereri from Germany, while all crypticus from Italy are found in the other group.

All other PCs explain less than 4.6% of the total variance. PC2 of the PCA based on genotype likelihoods separates nattereri-like animals from the Balkan peninsula (Albania, Bulgaria, Serbia, Bosnia and Herzegovina and Croatia) from individuals from Central Europe (Hungary and Germany) (Figure 1c). In contrast, PC2 of the PCA based on genotypes separates crypticus-like individuals along a geographic gradient from Central Italy to Hungary (Figure S1a).

Along the latter geographic transect, individuals appear slightly more similar to the group of nattereri-like individuals. The same transition among the crypticus-like individuals is also revealed by PC3 of both PCA approaches (Figure S2 for the genotype likelihood-based PCA and Figure S1b for the genotype-based PCA). Thus, both PCA approaches reveal that crypticus-like individuals become more similar to nattereri-like individuals (i.e. less separated along PC1) in the putative contact zone than outside of it.

### 3.3 | Admixture

The genetic structure of populations and the degree of admixture were analysed using two different data sets: first, using NGSAdmix for genotype likelihoods; and second, using Admixture for called genotypes. Both approaches suggested  $K=2$  as the optimal number of groups (Figure S3a,b) and led to an almost identical population structure. For  $K=2$ , the two main groups of the PCAs were recovered, that is, the nattereri-like and the crypticus-like individuals (Figure 1d, Figures S4 and S5). However, many individuals were identified as admixed individuals. Among the crypticus-like individuals, many had an admixture proportion of nattereri of ~15% and up to 30%. Such individuals were found in a confined geographic area comprising Croatia, Hungary and Bosnia-Herzegovina (Figure 1b). For  $K=3$ , these crypticus-like admixed individuals formed a separate group, likely indicating that their distinct genetic makeup is defined by their nattereri ancestry. For  $K=4$  and  $K=5$ , the nattereri-like individuals were split into a northern Central European population and a Balkan Peninsula population, which matches the grouping in the PCA.

Further inspection of the geographic origin of admixed individuals (Figure 1b, Table S1) revealed a rather homogenous group of admixed individuals in the south-western part of the Pannonian Basin. The admixture proportion of nattereri among 18 admixed individuals ranged between 10% and 17%. In addition, a single individual with a surprisingly high nattereri admixture proportion of 30% was found here. Along the edges of the Pannonian Basin, admixture proportions of nattereri either tend to decrease in the west (Eastern Alps and northern Dinaric Alps), that is, the transition zone to non-admixed crypticus-like individuals or increase in the north and east (Transdanubian and Carpathian Mountains), that is, transition zone to non-admixed nattereri-like individuals.

### 3.4 | Population differentiation

The differentiation between two populations ('pure nattereri' and 'pure crypticus') was investigated by the weighted Weir and Cockerham per site  $F_{ST}$  resulting in  $F_{ST}=0.46$ . Fixed differences ( $F_{ST}=1$ ) were found for 410,251 of the 25,788,685 SNPs sites (1.6%) investigated for this comparison. We also calculated nucleotide diversity ( $\pi$ ) for each of our pure populations. For the crypticus, the value was 0.0019, and for nattereri, the value was 0.00235.

Nucleotide divergence ( $D_{xy}$ ) was calculated to be 0.0042 between the pure populations.

Genome scans for all three parameters showed homogeneous patterns across scaffolds (Figure S6). The centromere region generally showed increased values in  $F_{ST}$  and lower values in  $D_{xy}$  and  $\pi$  in comparison to the arms of chromosomes.

### 3.5 | Ancestry informative markers (AIM)

Our AIM analysis considered only SNP sites that were fixed between 'pure nattereri' and 'pure crypticus'. Among the 410,251 fixed SNPs between the two groups, 267,348 to 410,147 fixed SNPs were called per individual. Within each admixed individual, the proportions of fixed SNPs of nattereri and crypticus, respectively, closely matched the admixture proportions of the two admixture analyses (Figures S4 and S5) and thus support the hybridization origin of admixed individuals. Heterozygosity was particularly high in one individual and close to 0.5, indicating a recent hybridization event. This animal was caught in Hungary among individuals with admixture proportions of ~15% nattereri and 85% crypticus. The triangle plot places this individual close to a first-generation backcross of an  $F_1$  to a crypticus individual (Figure 2). The similarity was even higher to a first-generation backcross of an  $F_1$  hybrid to the local hybrid population of 15% nattereri and 85% crypticus ancestry. In contrast, all other crypticus-like admixed individuals had values similar to those expected for individuals of a panmictic hybrid population with a 15% nattereri and 85% crypticus ancestry (Figure 2).

### 3.6 | Demographic history

We used two methods of demographic inference. First, we investigated the demographic history using a PSMC approach. Three individuals representing the three populations, 'pure nattereri' and 'pure crypticus' from northern Italy and 'pure crypticus' from southern Italy, were used (Figure 3). All three populations show similar periods of population expansion and decline. The first decline in the effective population size occurred around 600,000 to 300,000 years ago and is more prominent in the two crypticus populations than in the nattereri population. The peak effective population size was reached around 30,000 years ago for all three investigated populations. Subsequently, population size declined in all three populations, being more pronounced in nattereri than in crypticus. Also, the analysis shows that the effective population sizes for the crypticus populations (north and south) started to diverge around 22,000 years ago.

Second, five demographic scenarios, differing by gene flow patterns (no gene flow, early gene flow, different geneflow, constant gene flow and recent gene flow; Figure 4), were tested by continuous-time coalescent modelling implemented in Fastsimcoal2 (Excoffier et al., 2021). The recent gene flow model (secondary contact scenario) was supported best (Figure 4, Table S3), suggesting a split time between nattereri and crypticus of 3.6 (95% CI: 3.3–3.9) million years ago (MYA). The start of



**FIGURE 3** Pairwise sequential Markovian coalescent (PSMC) model for the three populations nattereri (orange), crypticus from southern Italy (grey) and crypticus from northern Italy (blue). Changes in effective population size  $N_e$  (with 100 bootstrap repetitions) in the three populations based on an autosomal pairwise sequential Markovian coalescent model. Generation time was set at 7.3 years and mutation rate per generation ( $\mu$ ) at  $2.5 \times 10^{-8}$ .

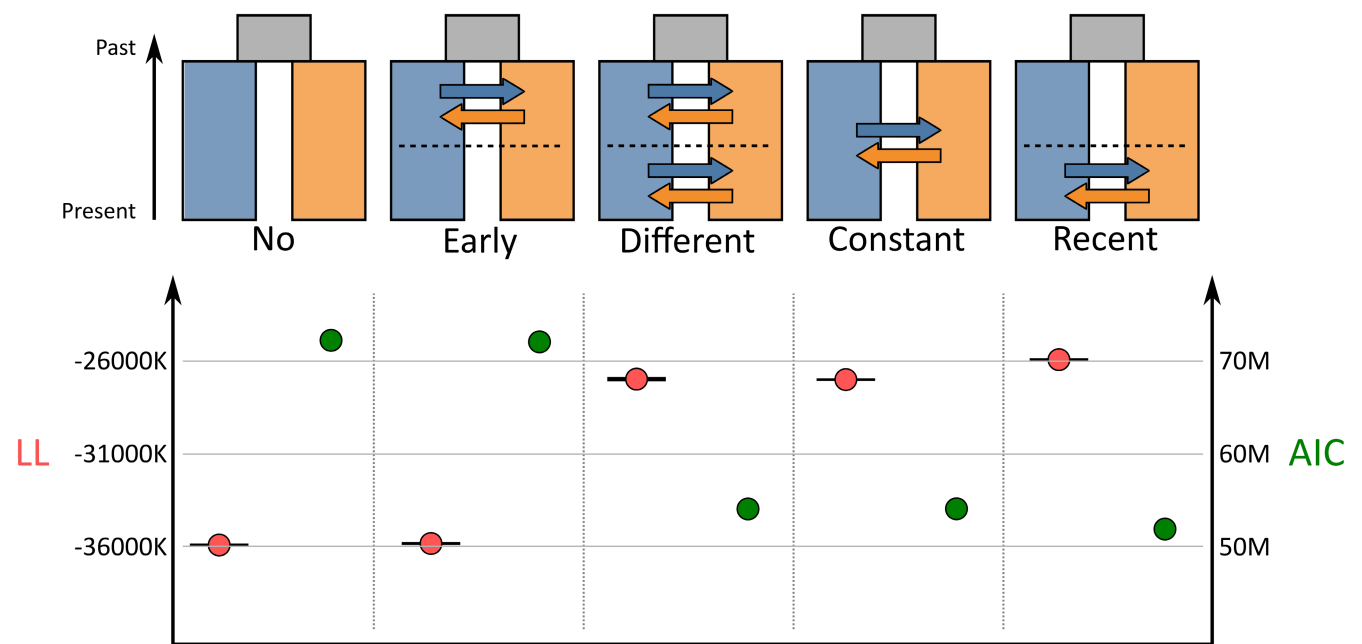
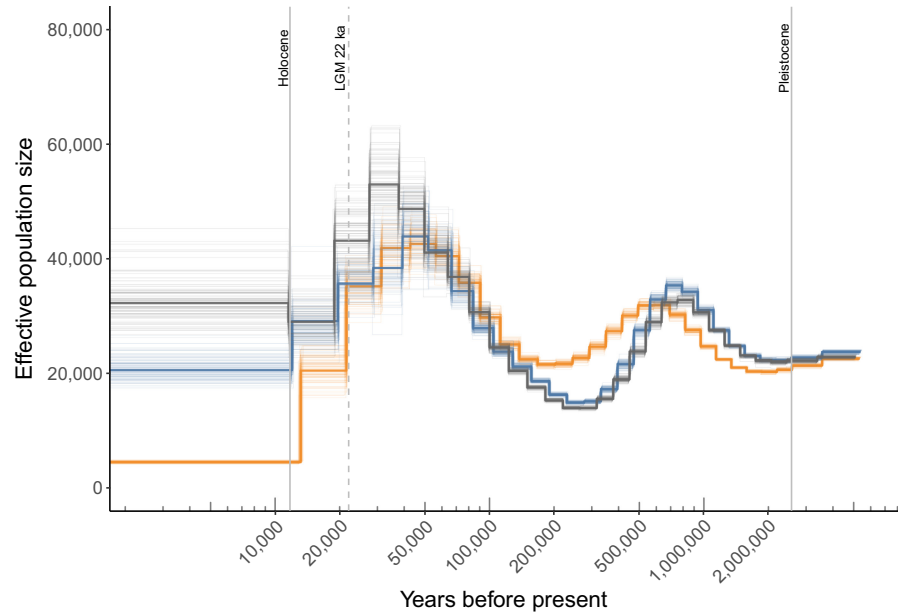


**FIGURE 4** Demographic models differing by gene flow on five scenarios were analysed by Fastsimcoal2. Fitting of the model simulations to our data set was evaluated by comparing Akaike information criteria (AIC, green circles) and log likelihoods (LL, red circles) of the five models.

the gene flow was estimated at 27 kYA (95% CI: 26–28) and population size estimates ( $2N$ ) differed between both species: 8226 (CI: 8160–8305) for crypticus and 10 (CI: 9–11) for nattereri. Migration measured as  $Nm$  was the same magnitude in both directions: 0.052 from nattereri to crypticus and 0.021 from crypticus to nattereri.

### 3.7 | Differentiation of the mitochondrial genome

In the mitochondrial DNA, we observed two highly distinct lineages, one representing the crypticus lineage and the other the nattereri

lineage (Figures 1a and 5). Within the crypticus lineage two highly divergent lineages were found, separating individuals from southern Italy from those in northern Italy, Austria, Slovenia and the northern Adriatic coast of Croatia. Within the nattereri lineage, a clear split occurs between individuals from the southern (Bulgaria, Albania, Serbia, Bosnia-Herzegovina and southern Croatia) and the northern distribution range (northern Croatia, Hungary and Germany) (Figure 5). This differentiation of the mitochondrial lineages agrees with the differentiation of the nuclear genome revealed by PCAs and admixture analyses. However, at an individual level, we observed conflicting assignments between the nuclear and the

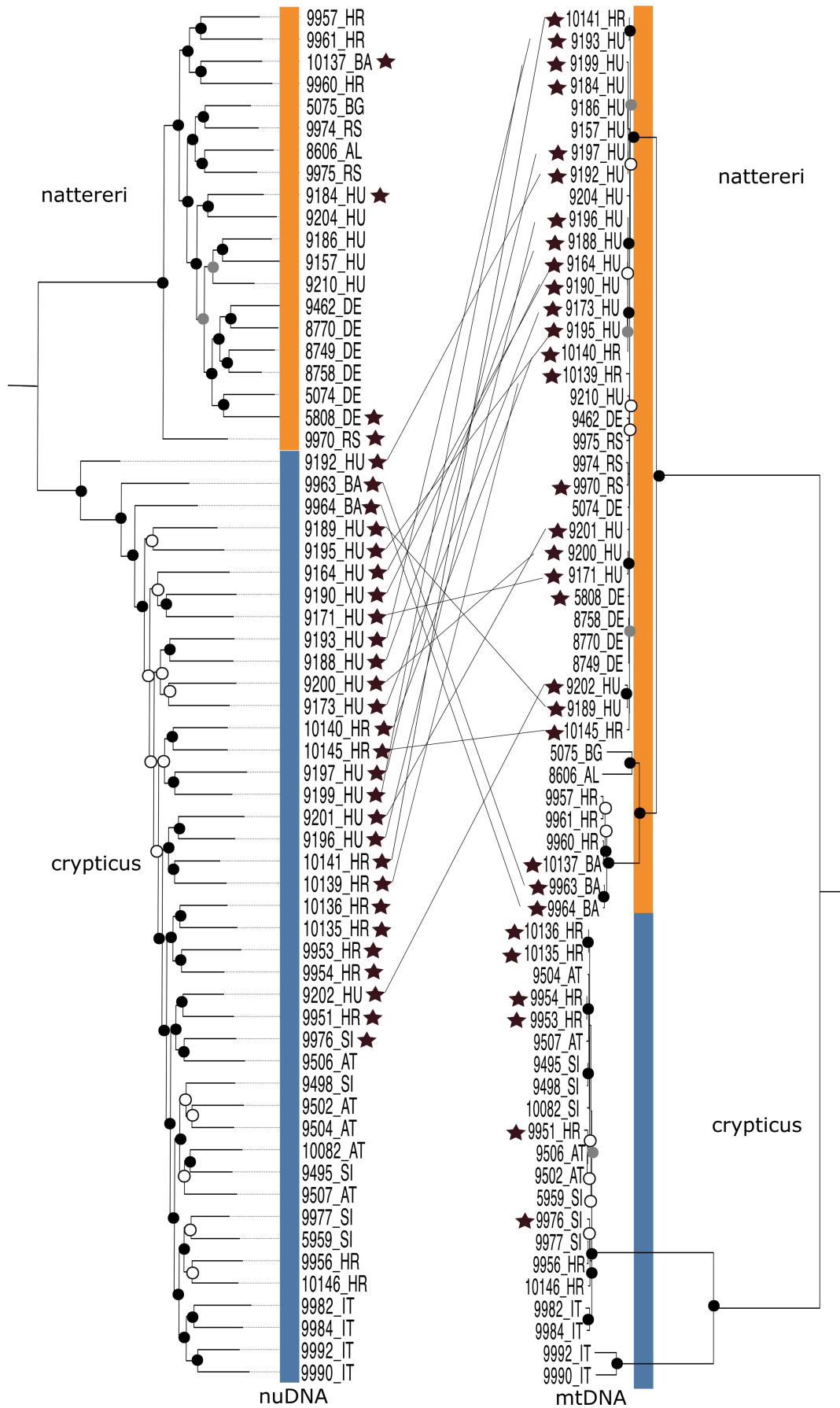


**FIGURE 5** Phylogenetic tree of nuclear and mitochondrial DNA. Blue are individuals of the crypticus lineage and orange are those of the nattereri lineage. Stars denote admixed individuals. Lines connecting both phylogenies refer to individuals with a mismatch between their nuclear and mitochondrial phylogenetic assignment. Circles at internal nodes indicate bootstrap support 50–70 (white), 70–90 (grey) and >90 (black). The name of each sample is followed by the abbreviation of the country where it was collected: Albania (AL), Austria (AT), Bosnia and Herzegovina (BA), Bulgaria (BG), Croatia (HR), Germany (DE), Hungary (HU), Italy (IT), Serbia (RS) and Slovenia (SI).

mitochondrial data (Figure 5). Among the 42 crypticus-like individuals, 21 (50%) carried a mitochondrial sequence of nattereri. All these 21 individuals were crypticus-like admixed individuals from Croatia, Bosnia-Herzegovina and Hungary. Only five crypticus-like admixed individuals carried a mitochondrial sequence of crypticus. The opposite mismatch was never observed.

## 4 | DISCUSSION

### 4.1 | Secondary contact

Whole-genome sequencing of 62 individuals from the *Myotis nattereri* species complex from Central Europe and the Apennine and Balkan Peninsulas revealed two genetically highly distinct lineages. These lineages lack obvious morphological differences and their external and craniodental traits largely overlap (Juste et al., 2018). One lineage was found on the Balkan Peninsula and in Central Europe representing the nattereri lineage, while the second lineage was found on the Apennine Peninsula, in the Eastern Alps and the northern Dinarides representing the crypticus lineage (Çoraman et al., 2019; Puechmaile et al., 2012; Ruedi et al., 2019; Salicini et al., 2013). Both lineages were separated geographically by mountain ranges (Alps) and the Mediterranean Sea and now form a wide contact zone in the eastern parts of the Alps and northern parts of the Dinarides. These results show that the two lineages represent unique gene pools with their own long-term evolutionary histories. In addition, our genomic approach also confirmed population divergence within the crypticus lineage separating into a northern and a southern population, which was so far only described based on mtDNA analysis (Salicini et al., 2011, 2013).

The contact zone is located in a well-known area of secondary contact zones of animals and plants, which resulted from post-glacial range expansions from glacial refugia on the Balkan and Apennine Peninsulas (Hewitt, 2000; Taberlet et al., 1998). Habitat diversity in this region is high, ranging from dry and open steppe habitats in the Pannonian Basin to wet and forested mountain regions in the Eastern Alps and Dinaric Alps. The interplay of ecological heterogeneity and genetic incompatibilities between lineages often gives rise to narrow contact and hybrid zones; a phenomenon observed in various other taxa in this region, such as *Triturus* newts (Arntzen et al., 2014), house mice (Macholán et al., 2011), *Hyla* frogs (Dufresnes et al., 2015) and *Bombina* fire-bellied toads (Dufresnes et al., 2020). In contrast, the contact zone of the nattereri and the crypticus lineages is exceptionally wide, spanning a gradual cline of more than 100km from Slovenia to Hungary. Not only the high mobility of bats but also the lack of effective hybridization barriers and minor or even no ecological differentiation between the two lineages have likely contributed to the large extent of this hybrid zone.

The contemporary contact zone was probably formed during the post-glacial warming in the Holocene, yet nattereri and crypticus diverged several million years ago in the Pliocene. Applying demographic modelling, we estimated a split time of c. 3.6 MYA (95% CI: 3.3–3.9 MYA) assuming a mutation rate of  $2.5 \times 10^{-8}$  (Sovic et al., 2016) and a generation time of 7.3 years (Fleischer et al., 2017). Both assumptions underlie some uncertainties since they were calculated for other organisms (humans and a closely related bat species). Our estimate is close to the prior estimates of c. 4 to 5 million years which were based on molecular phylogenies with fossil record calibrations (Morales et al., 2019; Ruedi et al., 2013). An earlier estimate of 1.2 MYA (Salicini et al., 2013) is likely caused by a too low mutation rate (see Puechmaile et al., 2012). Our estimates of divergence time are based on a human mutation rate (Nachman & Crowell, 2000), which was also employed in a study involving bats (Sovic et al., 2016). However, recent human mutation rate estimates are nearly twofold slower (1000 Genomes Project Consortium, 2010). Utilizing this revised estimate would consequently lead to a doubling of our divergence time estimates. Moreover, the generation time employed in our estimations originates from a congeneric species and may not accurately reflect that of our study group. The uncertainty of the parameters could impact the precision of our divergence time calculations. Nevertheless, all of these earlier or later divergence estimates argue for an ancient split.

The estimates for the divergence times of the nattereri and crypticus lineages resemble those of other taxa from the same region such as 4–5 MYA in *Triturus* newts (Wielstra, 2019) and c. 5 MYA in *Hyla* frogs (Dufresnes et al., 2015). Notably, all these estimates point to a period roughly after the Messinian salinity crisis event. This geological epoch is characterized by a significant drop in Mediterranean Sea levels. During this period, the disappearance of the Adriatic Sea created land bridges, likely facilitating gene flow between Apennine and the Balkan populations. Subsequently, c. 5.3 MYA, the refilling of the Mediterranean Basin during the Zanclean flood could have acted as a barrier, leading to the isolation of populations (Blanc, 2002).

The lack of any obvious external morphological differences between the nattereri and crypticus lineages (Çoraman et al., 2019; Juste et al., 2018) is surprising given a long time of divergence of both lineages. Insectivorous bats of the genus *Myotis* are a well-known example of adaptive morphological divergence when bats adapt to different ecological niches and might not diverge in morphology while occupying similar niches. However, stabilizing selection for specialized gleaning of insects in highly cluttered environments (Schnitzler & Kalko, 2001) likely prevented the nattereri and crypticus lineages from morphological divergence. Our own observations involving extensive mist netting as well as radiotelemetry support

this hypothesis. Both lineages were observed in a wide range of habitats ranging from dense forests to meadows (Dietz & Russo, unpublished). Maintaining the plesiomorphic state even over many million years likely happened also within the morphogroup of 'whiskered' bats. Two widely distributed European bat species *Myotis mystacinus* and *M. brandtii* remained unrecognized as distinct species until 1970 (Gaukler & Kraus, 1970; Hanák, 1970) illustrating their morphological similarity. Phylogenetic analyses surprisingly revealed that both species are representatives of the two most divergent clades within the morphologically highly diverse genus *Myotis* covering a time span of c. 30 MYA (Morales et al., 2019).

## 4.2 | Reproductive isolation

Despite the divergence between the *nattereri* and *crypticus* lineages c. 3.6 MYA, admixture analysis assigned individuals throughout the contact zone to both lineages (Figure 1b). In addition, a single individual from southern Bavaria exhibited an admixed genome as well, suggesting hybridization in multiple contact zones between the two lineages. Admixture proportions varied largely among individuals, suggesting extensive and ongoing hybridization between both lineages. Pure (non-admixed) individuals were either found on the Apennine Peninsula, in the Eastern Alps or the northwest of the Balkan Peninsula, representing the *crypticus* lineage or in the southern and eastern parts of the Balkan Peninsula and Central Europe representing the *nattereri* lineage.

Additional evidence for hybridization between both lineages comes from the frequent cyto-nuclear discrepancies in the Pannonian Basin and the southern Alps (see also Çoraman et al., 2019). Here, individuals showed a reverse representation of lineages in the nuclear and mitochondrial genome. For example, within the south-western Pannonian Basin, the mean admixture proportion of the *crypticus* nuclear genome was 85% (range from 70 to 93%), while 77% of these individuals (20 of 26) carried a mitochondrial genome of *nattereri*. The reverse pattern, that is, the introgression of a *crypticus* mitochondrial genome into an individual with a predominantly *nattereri* genome, was never observed. Such a cytonuclear conflict is usually explained by mitochondrial introgression from the local population into the range-expanding population (Berthier et al., 2006; Currat et al., 2008). Accordingly, *nattereri* settled first in the north-western Balkan Peninsula and *crypticus* expanded recently to this area.

Gene flow from *crypticus* into the population of the Pannonian Basin is indicated by the continuous distribution in combination with clinal transition from pure *crypticus* in Italy to the admixed population in the southwest of the Pannonian Basin (Figure 1b). Towards further East and North, the wide steppe habitats of the Little and Great Hungarian Plain represent an unsuitable habitat for bats of the *M. nattereri* complex (Boldogh et al., 2019; Zoltán, 2007). This region and Lake Balaton may impede gene flow between the admixed population in the southwestern Pannonian Basin and *nattereri* populations in the Carpathian Mountains and the southern Balkan Peninsula and thus can explain the lack of admixed individuals with

more even admixture proportions. However, gene flow seems to occur at least occasionally as indicated by one individual from the Pannonian Basin. Of 19 individuals analysed from this region, one expressed an admixture proportion of 70% *crypticus* and 30% *nattereri* (70/30%), while all other individuals showed admixture proportions close to 85/15%. This indicates the detection of a recent hybridization event since the high *nattereri* genome proportion in combination with the elevated rate of heterozygosity of this individual closely matches those of a first-generation backcross of an  $F_1$  hybrid with a local admixed individual (Figure 2).

Throughout our study area, we observed a strong genetic population structure. Within each confined geographic region, bats closely resembled each other genetically and differed to some degree from other regions. This was unexpected since bats are rather mobile and seasonal migration occurs between summer roosts and hibernation sites. In late summer and autumn, *M. nattereri* is known to gather at swarming sites like caves or mines during the mating period (Parsons & Jones, 2003; Rivers et al., 2006) where animals from different areas meet and mate (Pfeiffer & Mayer, 2013). Our findings suggest now that the catchment area of such swarming sites is rather regional, impeding gene flow across longer distances. This is in line with short dispersal and migration distances in *M. nattereri*. Banded bats of both sexes were usually recovered at distances below 50 km from the banding site (Hutterer, 2005; Rivers et al., 2006; Siemers et al., 1999).

Instead of finding evidence for reproductive isolation, we observed a wide hybrid zone with a clinal distribution of admixture proportions. A strikingly different pattern is observed in the sister group of *Myotis nattereri* group, that is, large *Myotis* species of the *Myotis myotis* complex. The sibling species *M. myotis* and *M. blythii* diverged within the last six MYA (Morales et al., 2019; Ruedi et al., 2013) and closely resemble each other in morphology, but have largely overlapping distribution ranges in Europe and Asia Minor. They occasionally even occur in the same roost. Here, hybridization is ongoing and causes asymmetrical introgression towards *M. blythii* (Afonso et al., 2017; Berthier et al., 2006). However, selection against hybrids likely prevents the collapse of species barriers (Berthier et al., 2006). The lack of a genomic analysis of hybridization between *M. myotis* and *M. blythii* limits a deeper understanding of the evolutionary consequences of hybridization between these taxa so far. However, their widely overlapping distribution ranges suggest effective barriers to gene flow, which led to their acceptance as good biological species. In contrast, the wide hybrid zone and clinal interbreeding patterns between *nattereri* and *crypticus* are best described by applying the subspecies concept (Mallet, 2001; Mayr, 1963) and treating the *crypticus* lineage as a (geographic) subspecies within the species *Myotis nattereri* (see also Çoraman et al., 2019).

The cryptic hybridization observed between the ancient lineages of the *Myotis nattereri* complex provides a compelling example of how the interplay of geography and the dynamic shifts in environmental conditions can produce complex patterns of genetic divergence and population structure. The lingering question pertains to the potential impacts of these hybridization events on the response of the species



to the challenges posed by current climate change. Monitoring this contact zone can offer unique insights into how evolutionary mechanisms such as introgression can change the fitness of individuals and thus can lead to rapid changes in population structures.

#### AUTHOR CONTRIBUTIONS

D.J., E.Ç., M.P.K.B. and F.M. designed the study. D.J., L.A., I.B., C.D., T.G., S.I.H.B., B.P., D.R., M.S. and V.Z. collected samples and did fieldwork. D.J., I.W. and S.I.H.B. did the DNA isolation and library preparation. S.F. sequenced the samples. D.J. and M.P.K.B. performed all the analyses. D.J. wrote a first draft of the manuscript with input from F.M. and E.Ç. All co-authors revised and accepted the manuscript.

#### ACKNOWLEDGEMENTS

The authors would like to thank Gábor Csorba, Imre Dombi, Péter Estók, Maria Jerabek, Marija Krajnović, Mirna Mazija, Jasminko Mulamerović, Guido Reiter, Dina Rnjak, Goran Rnjak and Nikola Tvrtković for their help with fieldwork. Also, we would like to thank Marie Gurke, Vanuhi Hambardzumyan, Elisabeth Hempel and Martina Nagy for their comments on the earlier versions of the manuscript. We would also like to thank Joshua V. Peñalba for his help with Fastsimcoal analysis. Also, Marie Gurke and Filip Thörn for their help with statistics and scripts. We are grateful to all people providing samples to earlier studies. These samples were partly used here and provided a valuable set of comparative data. The Bat1K Consortium kindly allowed us to use the genome of *Myotis myotis* prior to its publication. We would also like to thank to two anonymous reviewers and our handling editor for their help in greatly improving this manuscript. DNA samples originated from the DNA and tissue collection of the Museum für Naturkunde Berlin. Own fieldwork was carried out in Croatia during 2018 and 2019 under the permits Klasa UP/1-612/07/18-48/33 and UP/1-612-07/19-48/80. D.J. was funded by Elsa-Neumann-Scholarship Fund. T. G. was supported by the National Research, Development, and Innovation Fund of Hungary (NKFIH FK137778, RRF-2.3.1-21-2022-00010) and the János Bolyai Research Scholarship of the Hungarian Academy of Sciences (BO/00825/21). This study was financially supported by the Leibniz Association within the Leibniz Competition program (K309/2020). This work was supported by the Deutsche Forschungsgemeinschaft (project 407495230) as part of the Next Generation Sequencing Competence Network (project 423957469). Next Generation Sequencing was carried out at the Competence Centre for Genomic Analysis (Kiel) and at the Berlin Center for Genomics in Biodiversity Research (BeGenDiv). Open Access funding enabled and organized by Projekt DEAL.

#### CONFLICT OF INTEREST STATEMENT

The authors declare no competing interests.

#### DATA AVAILABILITY STATEMENT

The BioProject number of this project in GenBank is PRJNA909969. The complete mitochondrial genomes used in this paper are available

at GenBank under the accession nos. from OP919262 to OP919323. The untrimmed raw data were uploaded for all the individuals to the Sequence Read Archive under SAMN32108265 to SAMN32108326. Dryad repository with the filtered VCF file and three bam files used for the PSMC analyses can be found here <https://doi.org/10.5061/dryad.msbcc2g50>. Custom scripts used in this manuscript can be found here: [https://github.com/darijajosic/natterers\\_bats](https://github.com/darijajosic/natterers_bats).

#### BENEFIT-SHARING STATEMENT

A research collaboration was developed, collaborators are included as coauthors, the results of research have been shared with the provider communities and the broader scientific community (see above) and the research addresses a priority concern; in this case, the conservation of organisms was studied.

#### ORCID

Darija Josić  <https://orcid.org/0000-0002-8393-4970>

Frieder Mayer  <https://orcid.org/0000-0002-0594-9923>

#### REFERENCES

- 1000 Genomes Project Consortium. (2010). A map of human genome variation from population-scale sequencing. *Nature*, 467(7319), 1061–1073. <https://doi.org/10.1038/nature09534>
- Abbott, R., Albach, D., Ansell, S., Arntzen, J. W., Baird, S. J. E., Bierne, N., Boughman, J., Brelsford, A., Buerkle, C. A., Buggs, R., Butlin, R. K., Dieckmann, U., Eroukhanoff, F., Grill, A., Cahan, S. H., Hermansen, J. S., Hewitt, G., Hudson, A. G., Jiggins, C., ... Zinner, D. (2013). Hybridization and speciation. *Journal of Evolutionary Biology*, 26(2), 229–246. <https://doi.org/10.1111/j.1420-9101.2012.02599.x>
- Afonso, E., Goydadin, A.-C., Giraudoux, P., & Farny, G. (2017). Investigating hybridization between the two sibling bat species *Myotis myotis* and *M. blythii* from guano in a natural mixed maternity Colony. *PLoS One*, 12(2), e0170534. <https://doi.org/10.1371/journal.pone.0170534>
- Akaike, H. (1974). A new look at the statistical model identification. *IEEE Transactions on Automatic Control*, 19, 716–723.
- Alexander, D. H., Novembre, J., & Lange, K. (2009). Fast model-based estimation of ancestry in unrelated individuals. *Genome Research*, 19(9), 1655–1664. <https://doi.org/10.1101/gr.094052.109>
- Alexandrino, J., Baird, S. J. E., Lawson, L., Macey, J. R., Moritz, C., & Wake, D. B. (2005). Strong selection against hybrids at a hybrid zone in the *Ensatina* ring species complex and its evolutionary implications. *Evolution*, 59(6), 1334–1347. <https://doi.org/10.1111/j.0014-3820.2005.tb01783.x>
- Andrews, S. (2010). *FastQC: A quality control tool for high throughput sequence data* [Online].
- Arntzen, J. W., Wielstra, B., & Wallis, G. P. (2014). The modality of nine *Triturus* newt hybrid zones assessed with nuclear, mitochondrial and morphological data. *Biological Journal of the Linnean Society*, 113(2), 604–622. <https://doi.org/10.1111/bj12358>
- Artyushin, I. V., Bannikova, A. A., Lebedev, V. S., & Krusko, S. V. (2009). Mitochondrial DNA relationships among north Palaearctic Eptesicus (Vespertilionidae, Chiroptera) and past hybridization between common serotine and northern bat. *Zootaxa*, 52(2262), 40–52.
- Baiz, M. D., Tucker, P. K., & Cortés-Ortiz, L. (2019). Multiple forms of selection shape reproductive isolation in a primate hybrid zone. *Molecular Ecology*, 28(5), 1056–1069. <https://doi.org/10.1111/mec.14966>
- Barth, J. M. I., Gubili, C., Matschiner, M., Tørresen, O. K., Watanabe, S., Egger, B., Han, Y. S., Feunteun, E., Sommaruga, R., Jehle, R., &

- Schabetsberger, R. (2020). Stable species boundaries despite ten million years of hybridization in tropical eels. *Nature Communications*, 11(1), 1–13. <https://doi.org/10.1038/s41467-020-15099-x>
- Barton, N. H., & Hewitt, G. M. (1985). Analysis of hybrid zones. *Annual Review of Ecology and Systematics*, 16, 113–148. <https://doi.org/10.1146/annurev.es.16.110185.000553>
- Berthier, P., Excoffier, L., & Ruedi, M. (2006). Recurrent replacement of mtDNA and cryptic hybridization between two sibling bat species *Myotis myotis* and *Myotis blythii*. *Proceedings of the Royal Society B: Biological Sciences*, 273(1605), 3101–3109. <https://doi.org/10.1098/rspb.2006.3680>
- Blanc, P.-L. (2002). The opening of the Plio-quaternary Gibraltar Strait: Assessing the size of a cataclysm. *Geodinamica Acta*, 15(5–6), 303–317. <https://doi.org/10.1080/09853111.2002.10510763>
- Boldogh, S. A., Estók, P., Hegyi, Z., Dobrosi, D., Görföl, T., Bihari, Z., Dombi, I., Gombkötő, P., Paulovics, P., Mészáros, J., Máté, B., Bereczky, A., Szatyor, M., & Gécz, I. (2019). "Hogy vagytok denevérek?" – a monitorozó program első 15 évének néhány eredménye. In: O. Váczi, I. Varga, & B. Bakó (Eds.), *A Nemzeti Biodiverzitás-monitorozó Rendszer Eredményei II. – Gerinces Állatok* (pp. 93–117). Körös-Maros Nemzeti Park Igazgatóság (in English: "How are you, bats?" - the results of the first 15 years of the national bat monitoring programme).
- Bolger, A. M., Lohse, M., & Usadel, B. (2014). Trimmomatic: A flexible trimmer for Illumina sequence data. *Bioinformatics*, 30(15), 2114–2120. <https://doi.org/10.1093/bioinformatics/btu170>
- Chang, C. C., Chow, C. C., Tellier, L. C. A. M., Vattikuti, S., Purcell, S. M., & Lee, J. J. (2015). Second-generation PLINK: Rising to the challenge of larger and richer datasets. *GigaScience*, 4(1), 1–16. <https://doi.org/10.1186/s13742-015-0047-8>
- Chattopadhyay, B., Garg, K. M., Ray, R., & Rheindt, F. E. (2019). Fluctuating fortunes: Genomes and habitat reconstructions reveal global climate-mediated changes in bats' genetic diversity. *Proceedings of the Royal Society B: Biological Sciences*, 286(1911), 20190304. <https://doi.org/10.1098/rspb.2019.0304>
- Clare, E. L., Lim, B. K., Fenton, M. B., & Hebert, P. D. N. (2011). Neotropical bats: Estimating species diversity with DNA barcodes. *PLoS One*, 6(7), e22648. <https://doi.org/10.1371/journal.pone.0022648>
- Çoraman, E., Dietz, C., Hempel, E., Ghazaryan, A., Levin, E., Presetnik, P., Zagmajster, M., & Mayer, F. (2019). Reticulate evolutionary history of a Western Palaearctic bat complex explained by multiple mtDNA introgressions in secondary contacts. *Journal of Biogeography*, 46(2), 343–354. <https://doi.org/10.1111/jbi.13509>
- Çoraman, E., Dundarova, H., Dietz, C., & Mayer, F. (2020). Patterns of mtDNA introgression suggest population replacement in Palaearctic whiskered bat species: Population replacement in whiskered bats. *Royal Society Open Science*, 7(6), 191805. <https://doi.org/10.1098/rsos.191805>
- Çoraman, E., Furman, A., Karataş, A., & Bilgin, R. (2013). Phylogeographic analysis of Anatolian bats highlights the importance of the region for preserving the chiropteran mitochondrial genetic diversity in the Western Palaearctic. *Conservation Genetics*, 14(6), 1205–1216. <https://doi.org/10.1007/s10592-013-0509-4>
- Curat, M., Ruedi, M., Petit, R. J., & Excoffier, L. (2008). The hidden side of invasions: Massive introgression by local genes. *Evolution*, 62(8), 1908–1920. <https://doi.org/10.1111/j.1558-5646.2008.00413.x>
- Danecek, P., Auton, A., Abecasis, G., Albers, C. A., Banks, E., DePristo, M. A., Handsaker, R. E., Lunter, G., Marth, G. T., Sherry, S. T., McVean, G., & Durbin, R. (2011). The variant call format and VCFtools. *Bioinformatics*, 27(15), 2156–2158. <https://doi.org/10.1093/bioinformatics/btr330>
- Dietz, C., Gazaryan, A., Papov, G., Dundarova, H., & Mayer, F. (2016). *Myotis hajastanicus* is a local vicariant of a widespread species rather than a critically endangered endemic of the Sevan lake basin (Armenia). *Mammalian Biology*, 81(5), 518–522. <https://doi.org/10.1016/j.mambio.2016.06.005>
- Dufresnes, C., Brelsford, A., Crnobrnja-Isailović, J., Tzankov, N., Lymberakis, P., & Perrin, N. (2015). Timeframe of speciation inferred from secondary contact zones in the European tree frog radiation (*Hyla arborea* group). *BMC Evolutionary Biology*, 15(1), 155. <https://doi.org/10.1186/s12862-015-0385-2>
- Dufresnes, C., Pribille, M., Alard, B., Gonçalves, H., Amat, F., Crochet, P. A., Dubey, S., Perrin, N., Fumagalli, L., Vences, M., & Martínez-Solano, I. (2020). Integrating hybrid zone analyses in species delimitation: Lessons from two anuran radiations of the Western Mediterranean. *Heredity*, 124(3), 423–438. <https://doi.org/10.1038/s41437-020-0294-z>
- Evanno, G., Regnaut, S., & Goudet, J. (2005). Detecting the number of clusters of individuals using the software structure: A simulation study. *Molecular Ecology*, 14(8), 2611–2620. <https://doi.org/10.1111/j.1365-294X.2005.02553.x>
- Excoffier, L., Marchi, N., Marques, D. A., Matthey-Doret, R., Gouy, A., & Sousa, V. C. (2021). *fastsimcoal2*: Demographic inference under complex evolutionary scenarios. *Bioinformatics*, 37(24), 4882–4885. <https://doi.org/10.1093/bioinformatics/btab468>
- Fleischer, T., Gampe, J., Scheuerlein, A., & Kerth, G. (2017). Rare catastrophic events drive population dynamics in a bat species with negligible senescence. *Scientific Reports*, 7(1), 1–9. <https://doi.org/10.1038/s41598-017-06392-9>
- Furman, A., Çoraman, E., Çelik, Y. E., Postawa, T., Bachanek, J., & Ruedi, M. (2014). Cytonuclear discordance and the species status of *Myotis myotis* and *Myotis blythii* (Chiroptera). *Zoologica Scripta*, 43(6), 549–561. <https://doi.org/10.1111/zsc.12076>
- Garrison, E., & Marth, G. (2012). Haplotype-based variant detection from short-read sequencing. 1–9.
- Gaukler, A., & Kraus, M. (1970). Kennzeichen und Verbreitung von *Myotis brandti* (Eversman, 1845). *Zeitschrift fuer Saugetierkunde*, 35, 113–124.
- Hanák, V. (1970). Notes on the distribution and systematics of *Myotis mystacinus* Kuhl, 1819. *Bijdragen tot de Dierkunde*, 40(1), 40–44.
- Hanghøj, K., Moltke, I., Andersen, P. A., Manica, A., & Korneliussen, T. S. (2019). Fast and accurate relatedness estimation from high-throughput sequencing data in the presence of inbreeding. *GigaScience*, 8(5), giz034. <https://doi.org/10.1093/gigascience/giz034>
- Hewitt, G. (2000). The genetic legacy of the quaternary ice ages. *Nature*, 405(6789), 907–913. <https://doi.org/10.1038/35016000>
- Hewitt, G. M. (1988). Hybrid zones-natural laboratories for evolutionary studies. *Trends in Ecology & Evolution*, 3(7), 158–167. [https://doi.org/10.1016/0169-5347\(88\)90033-X](https://doi.org/10.1016/0169-5347(88)90033-X)
- Hutterer, R. (Ed.). (2005). *Bat migrations in Europe: A review of banding data and literature*. Federal Agency for Nature Conservation.
- Ibáñez, C., García-Mudarra, J. L., Ruedi, M., Stadelmann, B., & Juste, J. (2006). The Iberian contribution to cryptic diversity in European bats. *Acta Chiropterologica*, 8(2), 277–297. [https://doi.org/10.3161/1733-5329\(2006\)8\[277:TICTCD\]2.0.CO;2](https://doi.org/10.3161/1733-5329(2006)8[277:TICTCD]2.0.CO;2)
- Jebb, D., Foley, N. M., Kerth, G., & Teeling, E. C. (2017). The complete mitochondrial genome of the Bechstein's bat, *Myotis bechsteinii* (Chiroptera, Vespertilionidae). *Mitochondrial DNA Part B: Resources*, 2(1), 92–94. <https://doi.org/10.1080/23802359.2017.1280701>
- Jebb, D., Foley, N. M., Puechmaile, S. J., & Teeling, E. C. (2017). The complete mitochondrial genome of the greater Mouse-eared bat, *Myotis myotis* (Chiroptera: Vespertilionidae). *Mitochondrial DNA Part A: DNA Mapping, Sequencing, and Analysis*, 28(3), 347–349. <https://doi.org/10.3109/19401736.2015.1122775>
- Jebb, D., Huang, Z., Pippel, M., Hughes, G. M., Lavrichenko, K., Devanna, P., Winkler, S., Jermini, L. S., Skirmuntt, E. C., Katzourakis, A., Burkitt-Gray, L., Ray, D. A., Sullivan, K. A. M., Roscito, J. G., Kirilenko, B. M., Dávalos, L. M., Corthals, A. P., Power, M. L., Jones, G., ... Teeling, E. C. (2020). Six reference-quality genomes reveal evolution of bat adaptations. *Nature*, 583(7817), 578–584. <https://doi.org/10.1038/s41586-020-2486-3>

- Juste, J., Ruedi, M., Puechmaille, S. J., Salicini, I., & Ibáñez, C. (2018). Two new cryptic bat species within the *Myotis nattereri* species complex (Vespertilionidae, Chiroptera) from the Western Palearctic. *Acta Chiropterologica*, 20(2), 285. <https://doi.org/10.3161/15081109AC2018.20.2.001>
- Katoh, K., & Standley, D. M. (2013). MAFFT multiple sequence alignment software version 7: Improvements in performance and usability. *Molecular Biology and Evolution*, 30(4), 772–780. <https://doi.org/10.1093/molbev/mst010>
- Kindler, C., Chèvre, M., Ursenbacher, S., Böhme, W., Hille, A., Jablonski, D., Vamberger, M., & Fritz, U. (2017). Hybridization patterns in two contact zones of grass snakes reveal a new Central European snake species. *Scientific Reports*, 7(1), 1–12. <https://doi.org/10.1038/s41598-017-07847-9>
- Kopelman, N. M., Mayzel, J., Jakobsson, M., Rosenberg, N. A., & Mayrose, I. (2015). Clumpak: A program for identifying clustering modes and packaging population structure inferences across K. *Molecular Ecology Resources*, 15(5), 1179–1191. <https://doi.org/10.1111/1755-0998.12387>
- Korneliussen, T. S., Albrechtsen, A., & Nielsen, R. (2014). ANGSD: Analysis of next generation sequencing data. *BMC Bioinformatics*, 15(1), 1–13. <https://doi.org/10.1186/s12859-014-0356-4>
- Kruskop, S. V., & Solovyeva, E. N. (2020). Validating the relationships: Which species of *Myotis "nattereri"* group (Chiroptera: Vespertilionidae) actually inhabits the Caucasus. *Mammalia*, 85(1), 90–99. <https://doi.org/10.1515/mammalia-2019-0146>
- Leaché, A. D., & Cole, C. J. (2007). Hybridization between multiple fence lizard lineages in an ecotone: Locally discordant variation in mitochondrial DNA, chromosomes, and morphology. *Molecular Ecology*, 16(5), 1035–1054. <https://doi.org/10.1111/j.1365-294X.2006.03194.x>
- Li, H. (2011). A statistical framework for SNP calling, mutation discovery, association mapping and population genetical parameter estimation from sequencing data. *Bioinformatics*, 27(21), 2987–2993. <https://doi.org/10.1093/bioinformatics/btr509>
- Li, H., & Durbin, R. (2009). Fast and accurate short read alignment with Burrows–Wheeler transform. *Bioinformatics*, 25(14), 1754–1760. <https://doi.org/10.1093/bioinformatics/btp324>
- Li, H., & Durbin, R. (2011). Inference of human population history from individual whole-genome sequences. *Nature*, 475(7357), 493–496. <https://doi.org/10.1038/nature10231>
- Li, H., Handsaker, B., Wysoker, A., Fennell, T., Ruan, J., Homer, N., Marth, G., Abecasis, G., & Durbin, R. (2009). The sequence alignment/map format and SAMtools. *Bioinformatics*, 25(16), 2078–2079. <https://doi.org/10.1093/bioinformatics/btp352>
- Macholán, M., Baird, S. J. E., Dufková, P., Munclinger, P., Bimová, B. V., & Piálek, J. (2011). Assessing multilocus introgression patterns: A case study on the mouse x chromosome in central Europe. *Evolution*, 65(5), 1428–1446. <https://doi.org/10.1111/j.1558-5646.2011.01228.x>
- Mallet, J. (2001). Species, concepts of. *Encyclopedia of Biodiversity*, 5, 427–440.
- Mao, X., & Rossiter, S. J. (2020). Genome-wide data reveal discordant mitonuclear introgression in the intermediate horseshoe bat (*Rhinolophus affinis*). *Molecular Phylogenetics and Evolution*, 150, 106886. <https://doi.org/10.1016/j.ympev.2020.106886>
- Mayer, F., Dietz, C., & Kiefer, A. (2007). Molecular species identification boosts bat diversity. *Frontiers in Zoology*, 4, 1–5. <https://doi.org/10.1186/1742-9994-4-4>
- Mayr, E. (1963). *Animal species and evolution*. Harvard University Press. <https://doi.org/10.4159/harvard.9780674865327>
- McKenna, A., Hanna, M., Banks, E., Sivachenko, A., Cibulskis, K., Kernysky, A., Garimella, K., Altshuler, D., Gabriel, S., Daly, M., & DePristo, M. A. (2010). The genome analysis toolkit: A MapReduce framework for analyzing next-generation DNA sequencing data. *Genome Research*, 20(9), 1297–1303. <https://doi.org/10.1101/gr.107524.110>
- Meisner, J., & Albrechtsen, A. (2018). Inferring population structure and admixture proportions in low-depth NGS data. *Genetics*, 210(2), 719–731. <https://doi.org/10.1534/genetics.118.301336>
- Minh, B. Q., Schmidt, H. A., Chernomor, O., Schrempf, D., Woodhams, M. D., von Haeseler, A., & Lanfear, R. (2020). IQ-TREE 2: New models and efficient methods for phylogenetic inference in the genomic era. *Molecular Biology and Evolution*, 37(5), 1530–1534. <https://doi.org/10.1093/molbev/msaa015>
- Moore, W. S. (1977). An evaluation of narrow hybrid zones in vertebrates. *The Quarterly Review of Biology*, 52(3), 263–277. <https://doi.org/10.1086/409995>
- Morales, A. E., Ruedi, M., Field, K., & Carstens, B. C. (2019). Diversification rates have no effect on the convergent evolution of foraging strategies in the most speciose genus of bats, *Myotis*. *Evolution*, 73(11), 2263–2280. <https://doi.org/10.1111/evo.13849>
- Müllerbach, R., Lagoda, P. J., & Welter, C. (1989). An efficient salt-chloroform extraction of DNA from blood and tissues. *Trends in Genetics: TIG*, 5(12), 391.
- Nachman, M. W., & Crowell, S. L. (2000). Estimate of the mutation rate per nucleotide in humans. *Genetics*, 156(1), 297–304. <https://doi.org/10.1093/genetics/156.1.297>
- Okonechnikov, K., Conesa, A., & García-Alcalde, F. (2016). Qualimap 2: Advanced multi-sample quality control for high-throughput sequencing data. *Bioinformatics*, 32(2), 292–294. <https://doi.org/10.1093/bioinformatics/btv566>
- Parsons, K. N., & Jones, G. (2003). Dispersion and habitat use by *Myotis daubentonii* and *Myotis nattereri* during the swarming season: Implications for conservation. *Animal Conservation*, 6(4), 283–290. <https://doi.org/10.1017/S1367943003003342>
- Pfeiffer, B., & Mayer, F. (2013). Spermatogenesis, sperm storage and reproductive timing in bats. *Journal of Zoology*, 289(2), 77–85. <https://doi.org/10.1111/j.1469-7998.2012.00970.x>
- Phillips, B. L., Baird, S. J. E., & Moritz, C. (2004). When vicars meet: A narrow contact zone between morphologically cryptic phylogeographic lineages of the rainforest skink, *Carlia rubrigularis*. *Evolution*, 58(7), 1536–1548. <https://doi.org/10.1111/j.0014-3820.2004.tb01734.x>
- Puechmaille, S. J., Allegrini, B., Boston, E. S. M., Dubourg-Savage, M. J., Evin, A., Knochel, A., Le Bris, Y., Lecoq, V., Lemaire, M., Rist, D., & Teeling, E. C. (2012). Genetic analyses reveal further cryptic lineages within the *Myotis nattereri* species complex. *Mammalian Biology*, 77(3), 224–228. <https://doi.org/10.1016/j.mambio.2011.11.004>
- Puechmaille, S. J., Dool, S., Beuneux, G., & Ruedi, M. (2023). Newly described and already endangered: A new mammal species endemic to Corsica. *Revue Suisse de Zoologie*, 130(2), 335–351. <https://doi.org/10.35929/RSZ.0108>
- Rivers, N. M., Butlin, R. K., & Altringham, J. D. (2006). Autumn swarming behaviour of Natterer's bats in the UK: Population size, catchment area and dispersal. *Biological Conservation*, 127(2), 215–226. <https://doi.org/10.1016/j.biocon.2005.08.010>
- Ruedi, M., Puechmaille, S. J., Ibáñez, C., & Juste, J. (2019). Unavailable names in the *Myotis nattereri* species complex. *Journal of Biogeography*, 46(9), 2145–2146. <https://doi.org/10.1111/jbi.13665>
- Ruedi, M., Stadelmann, B., Gager, Y., Douzery, E. J. P., Francis, C. M., Lin, L. K., Guillén-Servent, A., & Cibois, A. (2013). Molecular phylogenetic reconstructions identify East Asia as the cradle for the evolution of the cosmopolitan genus *Myotis* (Mammalia, Chiroptera). *Molecular Phylogenetics and Evolution*, 69(3), 437–449. <https://doi.org/10.1016/j.ympev.2013.08.011>
- Salicini, I., Ibáñez, C., & Juste, J. (2011). Multilocus phylogeny and species delimitation within the Natterer's bat species complex in the Western Palearctic. *Molecular Phylogenetics and Evolution*, 61(3), 888–898. <https://doi.org/10.1016/j.ympev.2011.08.010>
- Salicini, I., Ibáñez, C., & Juste, J. (2013). Deep differentiation between and within Mediterranean glacial refugia in a flying mammal, the

- Myotis nattereri* bat complex. *Journal of Biogeography*, 40(6), 1182–1193. <https://doi.org/10.1111/jbi.12062>
- Schnitzler, H.-U., & Kalko, E. K. V. (2001). Echolocation by insect-eating bats. *Bioscience*, 51(7), 557. [https://doi.org/10.1641/0006-3568\(2001\)051\[0557:EBIEB\]2.0.CO;2](https://doi.org/10.1641/0006-3568(2001)051[0557:EBIEB]2.0.CO;2)
- Seehausen, O. (2006). Losing biodiversity by reverse speciation. *Current Biology*, 16(9), 334–337. <https://doi.org/10.1016/j.cub.2006.03.077>
- Sequeira, F., Alexandrino, J., Rocha, S., Arntzen, J. W., & Ferrand, N. (2005). Genetic exchange across a hybrid zone within the Iberian endemic golden-striped salamander, *Chioglossa lusitanica*. *Molecular Ecology*, 14(1), 245–254. <https://doi.org/10.1111/j.1365-294X.2004.02390.x>
- Siemers, B. M., Kaipf, I., & Schnitzler, H.-U. (1999). The use of day roosts and foraging grounds by Natterer's bats (*Myotis nattereri* KUHL, 1818) from a colony in Southern Germany. *Z Säugetierkd*, 64, 241–245.
- Singhal, S., & Moritz, C. (2013). Reproductive isolation between phylogeographic lineages scales with divergence. *Proceedings of the Royal Society B: Biological Sciences*, 280(1772), 20132246. <https://doi.org/10.1098/rspb.2013.2246>
- Skotte, L., Korneliussen, T. S., & Albrechtsen, A. (2013). Estimating individual admixture proportions from next generation sequencing data. *Genetics*, 195(3), 693–702. <https://doi.org/10.1534/genetics.113.154138>
- Slager, D. L., Epperly, K. L., Ha, R. R., Rohwer, S., Wood, C., Hemert, C., & Klicka, J. (2020). Cryptic and extensive hybridization between ancient lineages of American crows. *Molecular Ecology*, 29(5), 956–969. <https://doi.org/10.1111/mec.15377>
- Smirnov, D. G., Vekhnik, V. P., Dzhmirzoyev, G. S., & Titov, S. V. (2020). On the taxonomic status of species from the group *Myotis nattereri* (Chiroptera, Vespertilionidae) in the eastern Caucasus. *Nature Conservation Research*, 5(4), 30–42. <https://doi.org/10.24189/ncr.2020.052>
- Sovic, M. G., Carstens, B. C., & Gibbs, H. L. (2016). Genetic diversity in migratory bats: Results from RADseq data for three tree bat species at an Ohio windfarm. *PeerJ*, 2016(1), 1–16. <https://doi.org/10.7717/peerj.1647>
- Stamatakis, A. (2014). RAxML version 8: A tool for phylogenetic analysis and post-analysis of large phylogenies. *Bioinformatics*, 30(9), 1312–1313. <https://doi.org/10.1093/bioinformatics/btu033>
- Struck, T. H., Feder, J. L., Bendiksbj, M., Birkeland, S., Cerca, J., Gusarov, V. I., Kistenich, S., Larsson, K.-H., Liow, L. H., Nowak, M. D., Stedje, B., Bachmann, L., & Dimitrov, D. (2018). Finding evolutionary processes hidden in cryptic species. *Trends in Ecology & Evolution*, 33(3), 153–163. <https://doi.org/10.1016/j.tree.2017.11.007>
- Taberlet, P., Fumagalli, L., Wust-Saucy, A., & Cosson, J. (1998). Comparative phylogeography and postglacial colonization routes in Europe. *Molecular Ecology*, 7(4), 453–464. <https://doi.org/10.1046/j.1365-294x.1998.00289.x>
- Uvizl, M., & Benda, P. (2021). Diversity and distribution of the *Myotis nattereri* complex (Chiroptera: Vespertilionidae) in the Middle East: Filling the gaps. *Mammalian Biology*, 101(6), 963–977. <https://doi.org/10.1007/s42991-021-00143-0>
- Van der Auwera, G. A., Carneiro, M. O., Hartl, C., Poplin, R., Del Angel, G., Levy-Moonshine, A., Jordan, T., Shakir, K., Roazen, D., Thibault, J., Banks, E., Garimella, K. V., Altschuler, D., Gabriel, S., & DePristo, M. A. (2013). From fastQ data to high-confidence variant calls: The genome analysis toolkit best practices pipeline. *Current Protocols in Bioinformatics*, 43(1110), 11.10.1–11.10.33. <https://doi.org/10.1002/0471250953.bi1110s43>
- Wake, D. B., & Schneider, C. J. (1998). Taxonomy of the plethodontid salamander *Genus ensatina*. *Herpetologica*, 54(2), 279–298.
- Wielstra, B. (2019). Historical hybrid zone movement: More pervasive than appreciated. *Journal of Biogeography*, 46(7), 1300–1305. <https://doi.org/10.1111/jbi.13600>
- Wu, C. I. (2001). The genic view of the process of speciation. *Journal of Evolutionary Biology*, 14(6), 851–865. <https://doi.org/10.1046/j.1420-9101.2001.00335.x>
- Zhang, C., Rabiee, M., Sayyari, E., & Mirarab, S. (2018). ASTRAL-III: Polynomial time species tree reconstruction from partially resolved gene trees. *BMC Bioinformatics*, 19(S6), 153. <https://doi.org/10.1186/s12859-018-2129-y>
- Zhang, J., Kobert, K., Flouri, T., & Stamatakis, A. (2014). PEAR: A fast and accurate Illumina paired-end reAd mergeR. *Bioinformatics*, 30(5), 614–620. <https://doi.org/10.1093/bioinformatics/btt593>
- Zoltán, B. (2007). Horgasszörű denevér (*Myotis nattereri* Kuhl, 1819). In Z. Bihari, G. Csorba, & M. Heltai (Eds.), *Magyarország emlőseinek atlasza (Atlas of mammals in Hungary, In Hungarian)* (pp. 123–124). Budapest: Kossuth Kiadó.

## SUPPORTING INFORMATION

Additional supporting information can be found online in the Supporting Information section at the end of this article.

**How to cite this article:** Josić, D., Çoraman, E., Waurick, I., Franzenburg, S., Ancillotto, L., Bajić, B., Budinski, I., Dietz, C., Görföl, T., Hayden Bofill, S. I., Presetnik, P., Russo, D., Spada, M., Zrnčić, V., Blom, M. P. K., & Mayer, F. (2024). Cryptic hybridization between the ancient lineages of Natterer's bat (*Myotis nattereri*). *Molecular Ecology*, 33, e17411. <https://doi.org/10.1111/mec.17411>